Title

Exported plasmodial J domain protein, PFE0055c, and PfHsp70-x form a specific co-chaperone-chaperone partnership

Journal

Cell Stress and Chaperones, 26(2)

ISSN

1355-8145

Authors

Dutta, Tanima
Singh, Harpreet
Gestwicki, Jason E
et al.

Publication Date

2021-03-01

DOI

10.1007/s12192-020-01181-2

Peer reviewed

Cell Stress and Chaperones (2021) 26:355–366
https://doi.org/10.1007/s12192-020-01181-2

ORIGINAL PAPER

Exported plasmodial J domain protein, PFE0055c, and PfHsp70-x form a specific co-chaperone-chaperone partnership

Tanima Dutta [1,2] · Harpreet Singh [3] · Jason E. Gestwicki [4] · Gregory L. Blatch [1,2]

Received: 18 July 2020 / Revised: 6 November 2020 / Accepted: 13 November 2020 / Published online: 24 November 2020

Abstract

Plasmodium falciparum is a unicellular protozoan parasite and causative agent of a severe form of malaria in humans, accounting for very high worldwide fatality rates. At the molecular level, survival of the parasite within the human host is mediated by *P. falciparum* heat shock proteins (PfHsps) that provide protection during febrile episodes. The ATP-dependent chaperone activity of Hsp70 relies on the co-chaperone J domain protein (JDP), with which it forms a chaperone-co-chaperone complex. The exported *P. falciparum* JDP (PfJDP), PFA0660w, has been shown to stimulate the ATPase activity of the exported chaperone, PfHsp70-x. Furthermore, PFA0660w has been shown to associate with another exported PfJDP, PFE0055c, and PfHsp70-x in J-dots, highly mobile structures found in the infected erythrocyte cytosol. Therefore, the present study aims to conduct a structural and functional characterization of the full-length exported PfJDP, PFE0055c. Recombinant PFE0055c was successfully expressed and purified and found to stimulate the basal ATPase activity of PfHsp70-x to a greater extent than PFA0660w but, like PFA0660w, did not significantly stimulate the basal ATPase activity of human Hsp70. Small-molecule inhibition assays were conducted to determine the effect of known inhibitors of JDPs (chalcone, C86) and Hsp70 (benzothiazole rhodacyanines, JG231 and JG98) on the basal and PFE0055c-stimulated ATPase activity of PfHsp70-x. In this study, JG231 and JG98 were found to inhibit both the basal and PFE0055c-stimulated ATPase activity of PfHsp70-x. C86 only inhibited the PFE0055c-stimulated ATPase activity of PfHsp70-x, consistent with PFE0055c binding to PfHsp70-x through its J domain. This research has provided further insight into the molecular basis of the interaction between these exported plasmodial chaperones, which could inform future antimalarial drug discovery studies.

Keywords ATPase activity · Chalcone · Co-chaperone-chaperone complex · Heat shock protein · Plasmodial J domain protein · Rhodacyanine

Introduction

Plasmodium falciparum is known to be one of the most virulent species of protozoan parasite infecting humans, causing approximately 435,000 malaria deaths worldwide in 2017 (World Health Organization 2018). One family of proteins proposed to mediate survival of the parasite, and which consists of parasite-resident and exported members, are molecular chaperones, mainly heat shock proteins (Hsps) (Botha et al. 2007; Shonhai et al. 2007; Pesce and Blatch 2014). Besides protection of the parasite against the temperature fluctuations of febrile episodes, the major *P. falciparum* Hsps (PfHsps), especially PfHsp70 and PfHsp90, are involved in the pathological development of malaria (Shonhai et al. 2011; Njunge et al. 2013; Przyborski et al. 2015). Changes in the protein profile of parasites are one of the major challenges to the development of robust antimalarial drugs (Akide-Ndunge et al. 2009), and hence targeting PfHsp70s involved in protein folding and function could represent a new avenue for antimalarial drug development.

Hsp70s assist numerous protein-folding processes through their involvement with all major cellular chaperone systems

✉ Gregory L. Blatch
greg.blatch@nd.edu.au

[1] The Vice Chancellery, The University of Notre Dame Australia, Fremantle, WA, Australia

[2] The Institute for Immunology and Infectious Diseases, Murdoch University, Murdoch, WA, Australia

[3] Department of Bioinformatics, Hans Raj Mahila Maha Vidyalaya, Jalandhar, Punjab, India

[4] Department of Pharmaceutical Chemistry, University of California San Francisco, San Francisco, CA, USA

(Mayer and Bukau 2005). Hsp40s, the largest Hsp70 co-chaperone family, are ubiquitously expressed and involved in a range of cellular processes, co-opting and regulating Hsp70 to ensure that biological function is finely coordinated in space and time (Fan et al. 2003; Kampinga and Craig 2010; Cyr and Ramos 2015). All members have a signature J domain which consists of an HPD (histidine-proline-aspartate) motif and other critically conserved residues (Hennessy et al. 2000), and recently it was proposed that these co-chaperones be referred to as J domain proteins (JDPs; Kampinga et al. 2019). In addition to the J domain, other structural features of JDPs are a glycine/phenylalanine (GF)-rich region, a cysteine-rich region (zinc-binding domain), and a C-terminus for protein-protein interaction (Cheetham and Caplan 1998; Hennessy et al. 2005b), which have been used to classify them into types I to IV (Botha et al. 2007). Interaction and chaperone stimulation take place when a JDP binds to a short hydrophobic segment of the substrate protein and delivers it to Hsp70, with the HPD motif mediating stimulation of the Hsp70 ATPase activity, leading to stabilization of the substrate-bound chaperone state (Cheetham et al. 1994; Tsai and Douglas 1996). Detailed structural and functional studies of JDP-Hsp70 interaction have revealed that the J domain makes key contacts with the ATPase domain, the interdomain linker, and the substrate-binding domain (SDB) of Hsp70 (Gässler et al. 1998; Mayer et al. 1999; Genevaux et al. 2002; Hennessy et al. 2005a; Ahmad et al. 2011; Kumar et al. 2011; Kityk et al. 2018). Recently, novel insights were revealed into the molecular mechanism by which *Escherichia coli* JDP (EcDnaJ) stimulates the ATPase activity of *E. coli* Hsp70 (EcDnaK) by deducing the crystal structure of a J-domain-GF-EcDnaK fusion protein (Kityk et al. 2018). Structural and mutational analysis of the fusion construct highlighted critical residues involved in the EcDnaJ J domain interaction with the EcDnaK ATPase domain, interdomain linker, and SBD. Of particular relevance to our study, this structural analysis confirmed the important electrostatic interface between helix II of the J domain and lobe II of the EcDnaK ATPase domain involving key contacts R22-E206, R22-E217, K26-E217, and R27-D211, respectively.

The JDP family in *P. falciparum* comprises 49 members (PfJDPs), of which 19 are reported to be exported into the cytosol of host erythrocytes (Njunge et al. 2013). Out of six PfHsp70s of *P. falciparum* origin, only one (PfHsp70-x) has been found to be exported into the infected erythrocyte cytoplasm (Külzer et al. 2012; Grover et al. 2013). Although still limited, evidence is starting to emerge for PfJDP-Hsp70 chaperone partnerships within both the parasite and the host. The parasite-resident canonical type I PfJDP, PfHsp40/PF14_0359, has been shown to form a co-chaperone-chaperone partnership with PfHsp70-1 (Botha et al. 2011), which appears to be a more efficient chaperone machine than its human ortholog (Anas et al. 2020). The parasite-resident type II PfJDPs, Pfj4/ PFL0565w and PFB0595w, have also been shown to associate with PfHSp70-1 (Pesce et al. 2008; Njunge et al. 2015). All of these cytosolic parasite-resident PfJDPs showed increased expression under heat stress conditions (Pesce et al. 2008; Botha et al. 2011; Njunge et al. 2015).

The exported type II PfJDPs, PFE0055c and PFA0660w, have been shown to be exported into the erythrocyte cytosol and localized to J-dots along with PfHsp70-x (Külzer et al. 2010; Külzer et al. 2012; Grover et al. 2013). J-dots are highly mobile membranous structures which have been shown to contain *P. falciparum* erythrocyte membrane protein 1 (PfEMP1), suggesting that they play a role in the trafficking of this important virulence factor (Külzer et al. 2010; Külzer et al. 2012). Recently, Behl et al. (2019) demonstrated that PFA0660w comprises distinct cholesterol and substrate binding sites and that PfHsp70-x binds to cholesterol-bound PFA0660w and PfEMP1 simultaneously in vitro to form a complex. Biochemical studies indicated that PFA0660w could stimulate the ATPase activity of PfHsp70-x but not PfHsp70-1 and human Hsp70 (hHsp70) and that it was also highly effective in suppressing the aggregation of rhodanese (Daniyan et al. 2016). These findings indicated that PFA0660w could serve as a specific co-chaperone of PfHsp70-x and that it also had independent chaperone activity (Daniyan et al. 2016; Daniyan and Blatch 2017). The structure of the J domain of PFA0660w and the ATPase domain of PfHsp70-x and a model of a PFA0660w-J-domain-PfHsp70-x complex were recently reported (Day et al. 2019). These structural analyses suggested that residues towards the C-terminus of helix II of the J domain (including the HPD) formed the primary binding surface with the ATPase domain; however, the key contact residues in PfHsp70-x were not highlighted (Day et al. 2019). Also, the isolated J domains of PFA0660w and PFE0055c were shown to stimulate the ATPase activity of PfHsp70-x and to a lesser extent hHsp70, with maximal stimulation occurring at 10-20:1 co-chaperone-chaperone molar concentration (Day et al. 2019). Using a yeast two-hybrid system, Jha and co-workers also reported interactions between type II PfJDPs (PFA0660w, PFA0090c, PFE0055c, PF11_0099) and Hsp70s (hHsp70 and PfHsp70-1) (Jha et al. 2017). Interestingly, this yeast two-hybrid analysis showed an interaction between the exported type II PfJDPs and hHsp70 but not with PfHsp70-1 (Jha et al. 2017); however, the nature and affinity of the interactions were unclear, as the assay was an in vivo heterologous complementation system. A bioinformatics study reported that the specificity of JDP and PfHsp70-x interaction is likely to be independent of the J domain (Hatherley et al. 2014). This highlighted the importance of analysing full-length JDP and Hsp70 proteins in binding studies, as all protein domains will make a contribution to the structural features required for JDP-Hsp70 interaction.

Current antimalarial drugs are losing their effectiveness due to the development of parasite drug resistance. Heat shock proteins (PfHsp70s and PfJDPs) represent potential antimalarial drug targets (Pesce et al. 2010; Daniyan and Blatch 2017). In particular, PfHsp70-x knockout has been shown to compromise *P. falciparum* virulence (Charnaud et al. 2017), while PfHsp70-x knockdown has been found to cause a reduction in parasite growth under heat shock conditions that simulate febrile episodes (Day et al. 2019). Therefore, PfHsp70-x and PfHsp70-x-PFE0055c-PFA0660w J-dot complexes represent potential antimalarial drug targets. As a consequence, it has become imperative to study inhibitor compounds that modulate these PfHsp70-PfJDP complexes, in particular protein-protein interaction inhibitors. A number of small molecule compounds possessing antimalarial activity have been shown to inhibit the basal and JDP-stimulated ATPase activity of PfHsp70s, such as pyrimidinones (Chiang et al. 2009; Botha et al. 2011), bromo-β-lapachona (BBL) (Cockburn et al. 2011), and lapachol (Cockburn et al. 2014). Interestingly, malonganenone A (Mal A) which exhibits antimalarial activity but low cytotoxicity to human cell lines was shown to significantly inhibit the JDP-stimulated ATPase activity of PfHsp70-x but not that of hHsp70 (Cockburn et al. 2014). A number of natural and synthetic chalcones have been shown to possess antimalarial activity (Sinha et al. 2019; Qin et al. 2020); however, there have been limited studies on their JDP-Hsp70 inhibitor activity. Binding studies on various FLAG-tagged JDP proteins and mammalian castration-resistant prostate cancer (CRPC) cell lysates revealed that the chalcone C86 interacted specifically with the J domain and was an effective pan-inhibitor of JDPs (Moses et al. 2018). Rhodacyanines such as MK-077 and its analogues have been shown to be allosteric inhibitors of Hsp70, locking it in the ADP bound form, and thereby inhibiting nucleotide exchange and interfering with the binding of nucleotide exchange factors (NEFs) such as Bag (Rinaldi et al. 2018). It has also been reported that benzothiazole rhodacyanines, JG98, and another analogue, JG231, disrupted Hsp70-Bag protein-protein interactions in vitro and in animal cancer cell lines (Shao et al. 2018). Interestingly, benzothiazole rhodacyanines are known to have promising antimalarial activity (Pudhom et al. 2006). These small molecule inhibitors of human JDP and Hsp70 (C86, JG98, and JG231) have not been tested on parasitic JDP-Hsp70 systems and, therefore, represent potential molecular probes for characterizing parasitic chaperones.

Several exported PfJDPs have been reported; however, information related to their co-chaperone properties is scanty. While a number of detailed biochemical structural and functional studies have recently been conducted on PFA0660w (Daniyan et al. 2016; Behl et al. 2019; Day et al. 2019), similar studies have not been conducted on PFE0055c. We hypothesize that PFE0055c is a potential co-chaperone of PfHsp70-x and that it may also interact with hHsp70. Therefore, in the present study, we biochemically characterize the full-length exported type II JDP, PFE0055c, and also assess small molecule inhibitors for their effect on the basal ATPase activity and PFE0055c-stimulated ATPase activity of PfHsp70-x. This study provides further mechanistic insights into the function of these exported JDPs.

Materials and methods

Material

The inhibitors C86, JG231, and JG98 were prepared as previously described and provided as a gift for the purpose of testing their effect on the PfJDP-PfHsp70 chaperone system (Moses et al. 2018; Shao et al. 2018). All three inhibitors used in the current study were prepared in DMSO as 10 mM stocks and used in standard ATPase assays at a final concentration of 10 μM or as indicated for other assays.

Methods

The optimized coding sequence (for amino acids 63-402) for the expression of PFE0055c in *Escherichia coli* was synthesized and procured from GenScript (USA) with *Bam*HI and *Hind*III restriction endonuclease cleavage sites incorporated at the 5′ end and 3′ end of the nucleotide sequence, respectively. The optimized coding sequence of PFE0055c was inserted into a pQE30 expression vector to generate the pQE30-PFE0055c plasmid. The plasmids were transformed into *E. coli* M15 [pREP4] cells (Qiagen, Australia). The presence of the correct plasmid was validated by restriction digestion of the recombinant plasmids.

Heterologous expression and purification of PFE0055c

The full-length recombinant PFE0055c protein was expressed as a 6xHis fusion protein in *E. coli* M15 [pREP4] [pQE30-PFE0055c] after induction of cultures with 0.4-mM isopropyl-β-D-1-thiogalactopyranoside (IPTG) when A_{600} reached 0.4–0.6, followed by further incubation at 37 °C for 3 h with shaking. Bacterial cells expressing PFE0055c were harvested by centrifugation (10,000 g × 10 min at 4 °C). The cell pellet was resuspended in lysis buffer (LB-10 mM Tris-HCl, pH 8, 300 mM NaCl, 50 mM imidazole, 1 mM PMSF, 1 mg/ml lysozyme) and incubated for 30 min at room temperature, followed by sonication (30 s, pulse on/off). The suspension was clarified by centrifugation at 12,000 g for 20 min at 4 °C, followed by washing the pellet with pellet wash buffer (PWB-50 mM Tris-HCl pH 8, 200 mM NaCl, 10 mM EDTA, 1% triton-X 100, 1 mM PMSF). Pellets were washed twice

with PWB and once with autoclaved double distilled water. The pellet was recovered after every wash by centrifugation (10,000 g, 10 min at 4 °C). The pellet was then resuspended in solubilization buffer (SB-10 mM Tris-HCl pH 8, 300 mM NaCl, 8 M urea, 50 mM imidazole, 5 mM DTT, 0.1 mM EDTA, 1 mM PMSF) and the pellet recovered by centrifugation at 12,000 g for 20 min at 4 °C. For purification and refolding, the supernatant was collected and further diluted to 250 μg/ml with refolding buffer (RB-100 mM Tris-HCl pH 8, 300 mM NaCl, 0.1 mM EDTA, 1 mM PMSF, 2 M urea, 50 mM imidazole, 1 mM DTT, 0.1% PEG 2000, 10% glucose, 5% sucrose). Diluted supernatant containing the recombinant protein was filtered using a 0.45-μM filter before adding to Ni-NTA slurry (Qiagen, Australia) and incubating on rotator at slow speed for 2 h at 4 °C. This was then loaded onto a column and washed with three-bed volumes of RB without urea and subsequently twice with RB without urea and PEG. Matrix-bound protein was eluted three to five times by addition of one-bed volume of elution buffer (EB-50 mM Tris-HCl pH 8, 2 mM $MgCl_2$, 100 mM KCl, 250 mM imidazole). The EB was adapted from a buffer previously developed for the purification of PFA0660w (Daniyan et al. 2016) with addition of $MgCl_2$ and KCl to be compatible with the ATPase assay. The purified recombinant protein was analysed by 12% sodium dodecyl sulphate-polyacrylamide gel electrophoresis (SDS-PAGE) and visualized following coomassie brilliant blue (CBB) staining and destained using 20% methanol (Sambrook and Russell 2001). The purification of (His_6)-PfHsp70-x (native conditions) using plasmid pQE30-PfHsp70-x, (His_6)-hHsp70 (native conditions) using plasmid pMSHsp70, and (His_6)-PFA0660w (denaturing conditions similar to the purification of PFE0550c) using plasmid pQE30-PFA0660w was performed as previously described (Chiang et al. 2009; Cockburn et al. 2011; Cockburn et al. 2014; Daniyan et al. 2016).

ATPase assays

The concentration of the purified recombinant proteins was estimated by the Bradford method (Bradford 1976). Steady-state ATPase assays were carried out according to the manufacturer's instructions for a high-throughput colorimetric ATPase assay kit (Innova Biosciences, UK). The 200-μl assay mixture contained 100-μl substrate buffer (SB-0.5 M Tris buffer, 0.1 M $MgCl_2$, 10 mM ATP). The assay procedure was started by mixing 100 μl of SB with 100 μl of Hsp70 and/or JDP (in EB-50 mM Tris-HCl pH 8, 2 mM $MgCl_2$, 100 mM KCl, 250 mM imidazole). The reaction was incubated for 1 h at 37 °C and then stopped by addition of 50 μl of Pi ColorLock mix (freshly prepared). After 2 min, a 20-μl stabilizer reagent was added to the reaction, resulting in a green colour developing for samples with Pi. The change in absorbance at 595 nm was monitored using a spectrophotometer (SPECTRO star Omega, BMG Labtech, Australia). The absorbance values for samples were used to determine μM Pi from a Pi standard curve. Equimolar concentrations (0.4 μM) of JDP and Hsp70s were used to assay the basal and stimulated ATPase activities of chaperones. A range of increasing concentrations of PFE0055c was employed to determine the specificity of the stimulation of the ATPase activity of PfHsp70-x and hHsp70. The effect of inhibitors (C86, JG231, and JG98) was studied by determining the inhibition of the basal and stimulated ATPase activities of chaperones. The inhibitors (10 μM) were added to the assay mix containing chaperone and co-chaperone (0.4 μM each), followed by incubation at room temperature for 10 min before the start of reaction by addition of ATP. Blank and control reactions were conducted with equal volume of elution buffer (for purified protein) and DMSO (for inhibitor), respectively. Assays were conducted in triplicate, and three separate experiments were performed using batches of independently purified proteins. The ATPase activity was expressed as nmol Pi/min and percent fold increase. Data were expressed as the mean ± standard error of the mean (mean ± SEM).

Bioinformatics analysis

Multiple sequence alignments of the PFE0055c and PFA0660w J domains were performed using the online clustalw server (https://www.ebi.ac.uk/Tools/msa/clustalw2/). Comparative modelling of the J domains of PFE0055c and PFA0660w were performed with Modeller 9.12. Graphical images of structural features were obtained with UCSF chimera 1.10.1 molecular visualization tool (Pettersen et al. 2004). For the present study, the PfHsp70-x ATPase domain structure (PDB ID: 6S02) was remodelled for missing residues (at position 217–221) in accordance with crystal structure of EcDnaK (PDB ID: 5NRO) (Kityk et al. 2018). Docking studies of the J domains of PFE0055c and PFA0660w with the ATPase domain of PfHsp70-x and hHsp70 were performed using the HADDOCK2.2 Server (https://alcazar.science.uu.nl/enmr/services/HADDOCK2.2/) (Van Zundert et al. 2016). The electrostatic and van der Waals energy were calculated using OPLS (optimized potentials for liquid simulations) force field. The HADDOCK score is derived by combining these energy terms along with additional empirical terms (desolvation, buried surface area) and restraint violation energies using a formula which included weightings for the different terms (Van Zundert et al. 2016). Detailed interaction maps of interacting sites for the J domains of PFA0660 and PFE0055c with the ATPase domains of PfHsp70-x and hHsp70 were obtained with LigPlot+ (https://www.ebi.ac.uk/thornton-srv/software/LigPlus/) (Laskowski and Swindells 2011).

Result and discussion

PFE0055c was reported to be exported to J-dot complexes with PFA0660w and PfHsp70-x (Külzer et al. 2012), suggesting a possible functional interaction. Therefore, here we conducted a biochemical characterization of the structural and functional properties of PFE0055c.

Alignment of PfJDPs suggests distinct interactions of PFE0055c and PFA0660w with Hsp70s

Despite the high sequence similarity between PFA0660w and PFE0055c, multiple sequence alignment (Fig. 1a) and three-dimensional (3D) models (Fig. 1b) of the J domains elucidated difference in critical residues responsible for interaction with Hsp70. Arginine (R101), leucine (L103), and lysine (K26) in the J domains of PFE0055c, PFA0660w and EcDnaJ, respectively, are highlighted, showing that PFE0055c (like EcDnaJ) has the conserved positively charged residue (R or K) typically required at this position for functional interaction with Hsp70 (Hennessy et al. 2005a; Nicoll et al. 2007), while PFA0660w has a non-conserved hydrophobic residue likely to disrupt interaction with Hsp70. There are a limited number of examples of other JDPs with a non-conserved residue at this position in the J domain, and none has been biochemically characterized (e.g. the yeast JDP ScJjj2 also has L at this position; Gillies et al. 2012). These structural differences prompted us to biochemically characterize PFE0055c and analyse any co-chaperone-chaperone complex formation with PfHsp70-x and hHsp70. Heterologous expression of recombinant $(His)_6$-PFE0055c was successfully achieved in *E. coli* M15 [pREP4] [pQE30-PFE0055c], which was the first step towards the analysis of the functional properties of PFE0055c.

While the solubility assay revealed that the induced PFE0055c protein was insoluble and present in inclusion bodies, it was successfully purified using solubilization and refolding buffers (Bondos and Bicknell 2003; Swietnicki 2006). Resolution by SDS-PAGE revealed a single band of 42 kDa in the eluted fractions for PFE0055c (Fig. 1c), implying that the recombinant protein had been successfully refolded and purified. This is the first report of the recombinant expression and purification of PFE0055c.

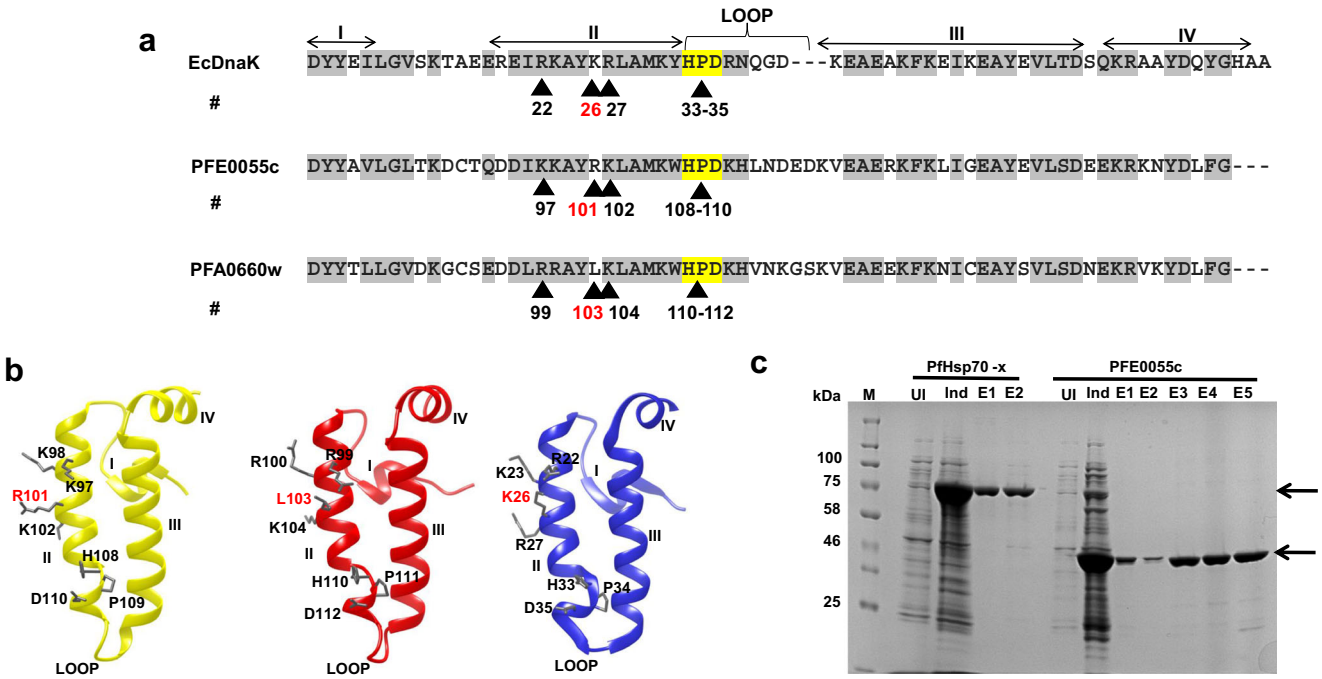

Fig. 1 Sequence analysis of the J domains of PFE0055c and PFA0660w and purification of PfHsp70-x and PFE0055c. (a) Multiple sequence alignment of the PFE0055c, PFA0660w, and EcDnaJ J domains. The HPD motifs are highlighted in yellow, similar amino acids are highlighted in grey, the protein helices and loop regions are defined by bidirectional arrows on top of the alignment, and critical amino acids are numbered and identified by arrowheads. The amino acid numbering for each J domain represents the positions of residues in the respective proteins. (b) Homology models of the J domains of PFE0055c (yellow), PFA0660w (red), and EcDnaJ (blue) to illustrate some differences in the conserved residues critical for protein-protein interaction. The models were prepared employing Modeller 9.12 and graphically rendered using UCSF Chimera 1.10.1. (c) SDS-PAGE gel of the purification of PfHsp70-x and PFE0055c. Total protein was isolated from *E. coli* M15 [pREP4] [pQE30-PfHsp70-x] and *E. coli* M15 [pREP4] [pQE30-PFE0055c] before (UI) and after induction (Ind) with IPTG, and purified protein eluted (E1-E2 for PfHsp70-x under native conditions; and E1-E5 for PFE0055c under denaturing and refolding conditions) after Ni-NTA affinity chromatography. Arrows indicate the purified recombinant proteins. The protein molecular mass markers are represented in kilo Daltons (kDa)

PFE0055c selectively stimulated the ATPase activity of PfHsp70-x

The ability of PFE0055c to stimulate the ATPase activity of PfHsp70-x and other likely chaperone partners, such as hHsp70, was determined. Both PfHsp70-x and hHsp70 were purified under native conditions and assessed to be functionally active as they had normal basal ATPase activity that could be stimulated by JDPs, as described here (Fig. 2). PFE0055c was observed to significantly stimulate the ATPase activity of PfHsp70-x by at least threefold ($P < 0.05$) at equimolar concentrations (0.4 μM), whereas the fold change in the ATPase activity of hHsp70 in the presence of PFE0055c was not significant (Fig. 2a). At equimolar concentrations, PFA0660w stimulated the ATPase activity of PfHsp70-x (1.5-fold change) and hHsp70 (1.2-fold change) (Fig. 2b) similarly to an earlier report (Daniyan et al. 2016). No ATPase activity was ever observed for PFE0055c or PFA0660w alone. Overall, these data indicated that PFE0055c selectively stimulated the ATPase activity of PfHsp70-x to a greater extent than PFA0660w (Fig. 2a and b). This could be attributed to the structural differences in conserved residues within their J domains (e.g. the R101 versus L103 on the J domain of PFE0055c and PFA0660w, respectively). The residue L103 in PFA0660w is an atypical amino acid for this position in the J domains of most JDPs (Hennessy et al. 2000), which could lead to a more hydrophobic low affinity binding surface being presented to interacting partner Hsp70s. Therefore, we hypothesize that PfHsp70-x-PFE0055c chaperone-co-chaperone complexes could have a higher order of affinity than PfHsp70-x-PFA0660w complexes. To further understand the PFE0055c selectivity for chaperone partner proteins (PfHsp70-x and hHsp70), ATPase assays were performed with increasing concentration of PFE0055c (0–2 μM) while keeping the Hsp70 concentration constant (0.4 μM). It was observed that with increasing PFE0055c concentration, the ATPase activity of PfHsp70-x increased proportionally, with saturation at high PFE0055c concentration (above 1.0 μM), whereas no increase or saturation was observed for the ATPase activity of hHsp70 (Fig. 2c). These findings indicate

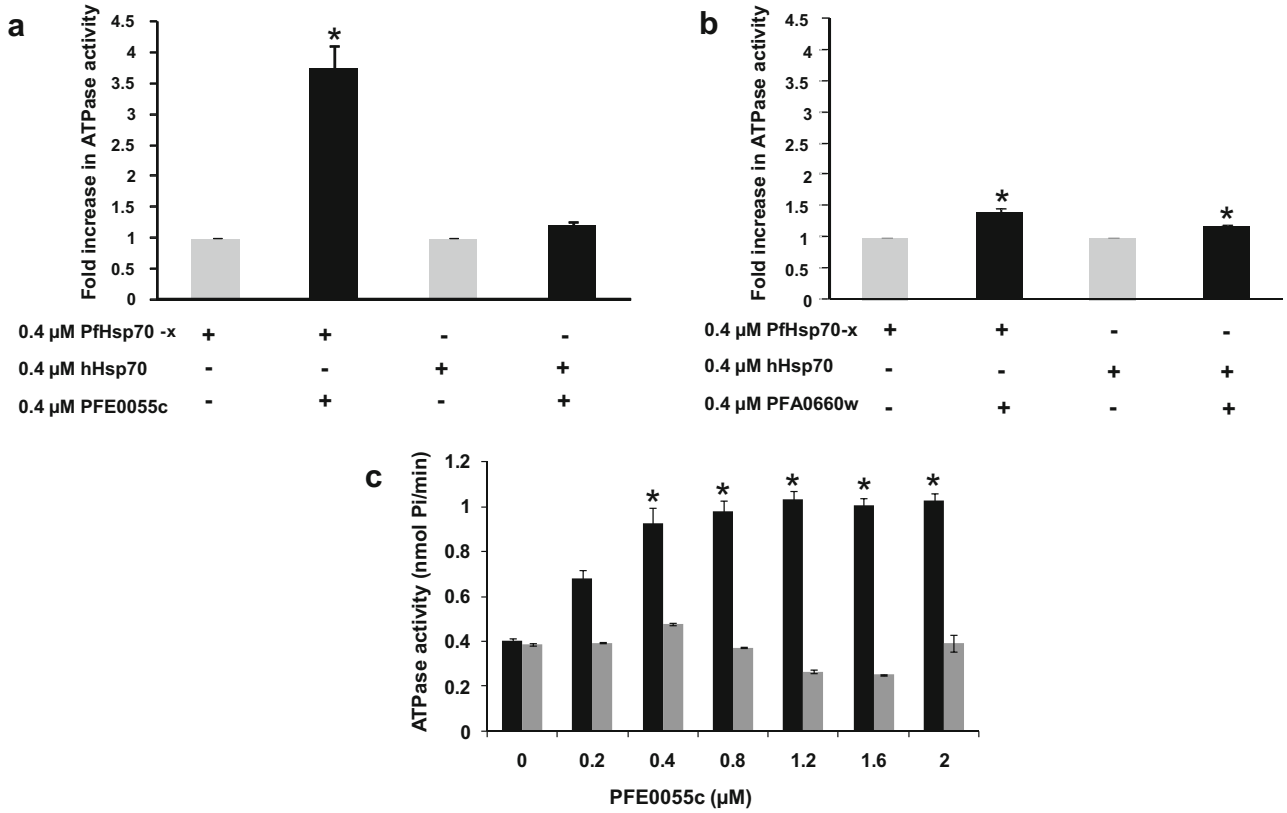

Fig. 2 PFE0055c selectively stimulates the ATPase activity of PfHsp70-x. (a) The bar graphs show the basal (grey; set as 1.0) and fold increase in PFE0055c-stimulated (black) ATPase activities of PfHsp70-x and hHsp70 expressed as the mean ± SEM. (b) The bar graphs show the basal (grey; set as 1.0) and fold increase in PFA0660w-stimulated (black) ATPase activities of PfHsp70-x and hHsp70 expressed as the mean ± SEM. In A and B, constituents that were either included or omitted from the reaction medium are indicated by (+) or (−) signs, respectively. Shown here are the combined data from three independent experiments performed in triplicate using independently purified proteins for each experiment. (c) The bar graphs show the stimulation of the basal ATPase activity of PfHsp70-x (0.4 μM; black) and hHsp70 (0.4 μM; grey) with increasing concentrations of PFE0055c (0–2 μM) expressed as the mean ± SEM. Error bars are indicated and an asterisk (*) indicates statistical significance at $P < 0.05$ relative to the basal ATPase value for the respective chaperone using the Student *t* test. Shown here are the combined data from at least two independent experiments performed in triplicate using independently purified proteins for each experiment

that PFE0055c is selective in its interaction with PfHsp70-x, suggesting PFE0055c could be a dedicated co-chaperone of PfHp70-x. However, further studies using a range of other potential Hsp70 partner proteins would need to be conducted to confirm the degree of selectivity.

The PFE0055c-stimulated PfHsp70-x ATPase activity could be specifically inhibited by a J domain-specific pan-inhibitor

The chalcone C86 has been shown to bind specifically to the J domain and to be a pan-inhibitor of JDPs (Moses et al. 2018), while the benzothiazole rhodacyanines JG98 and JG231 have been shown to be allosteric inhibitors of Hsp70, locking it in the ADP bound form, and thereby inhibiting nucleotide exchange (Rinaldi et al. 2018; Shao et al. 2018). We tested these specific inhibitors for their effect on the basal and PFE0055c-stimulated ATPase activity of PfHsp70-x, knowing their specific sites of interaction (Fig. 3a). The chalcone C86 was tested in PfHsp70-x ATPase activity assays in the absence and presence of PFE0055c (Fig. 3b). Reaction constituents were added in various orders and combinations to fully assess inhibition. It was observed that C86 has no effect on the basal ATPase activity of PfHsp70-x (Fig. 3b). ATPase assays revealed that C86 did not significantly inhibit PFE0055c-stimulated ATPase activity of PfHsp70-x when added to pre-incubated PFE0055c and PfHsp70-x, whereas significant inhibition was observed when C86 was pre-incubated with PFE0055c prior to the addition of PfHsp70-x (Fig. 3b). This was done to confirm total inhibition of basal and stimulated ATPase activity of PfHsp70-x (Fig. 3b). Since C86 is known to be a JDP pan-inhibitor that specifically binds the J domain (Moses et al. 2018), this finding indicated that the interaction of PFE0055c with PfHsp70-x was J domain–based. In similar experiments, the ATPase assay was conducted employing JG98 and JG231 for inhibition studies. We observed that JG98 and JG231 inhibited basal- and PFE0055c-stimulated ATPase activity of PfHsp70-x (Fig. 3c and d). This was consistent with earlier reports that JG231 and JG98 compounds inhibited nucleotide exchange by locking Hsp70 in the ADP bound form (Rinaldi et al. 2018; Shao et al. 2018; Gestwicki and Shao 2019).

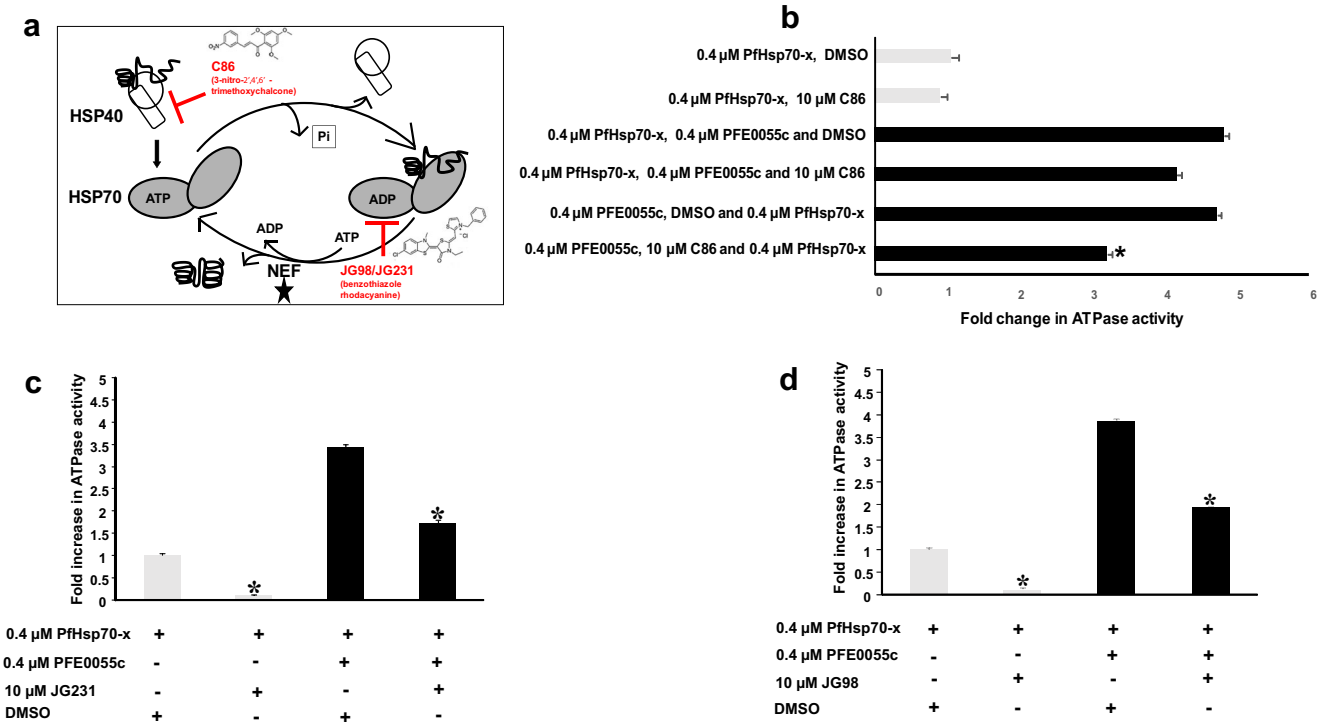

Fig. 3 Effect of inhibitors on basal and PFE0055c-stimulated PfHsp70-x ATPase activity. (a) Schematic diagram of the nucleotide-dependent Hsp70 substrate binding and release cycle, showing that the allosteric inhibitors JG98 and JG231 lock Hsp70 in the ADP bound form, thereby inhibiting nucleotide exchange (promoted by nucleotide exchange factors, NEFs) and the JDP pan-inhibitor C86 which specifically binds to the J domain. (b) C86 inhibited only PFE0055c-stimulated PfHsp70-x ATPase activity. The grey bars represent basal ATPase activity for PfHsp70-x (set as 1.0 for PfHsp70-x DMSO) in comparison to black bars representing fold increase in PFE0055c-stimulated activity. The *Y*-axis legend indicated the order in which reaction constituents were added. (c) JG231 and (d) JG98 inhibited basal and PFE0055c-stimulated PfHsp70-x ATPase activity. The bar graphs show the basal (set a 1.0 for PfHsp70-x DMSO) and fold increase in PFE0055c-stimulated ATPase activities of PfHsp70-x expressed as mean ± SEM. Error bars are indicated on each bar and the asterisk (*) indicates statistical significance at $P < 0.05$ relative to the basal ATPase value using the Student *t* test. Shown here are the combined data from at least three independent experiments performed in triplicate using independently purified proteins for each experiment

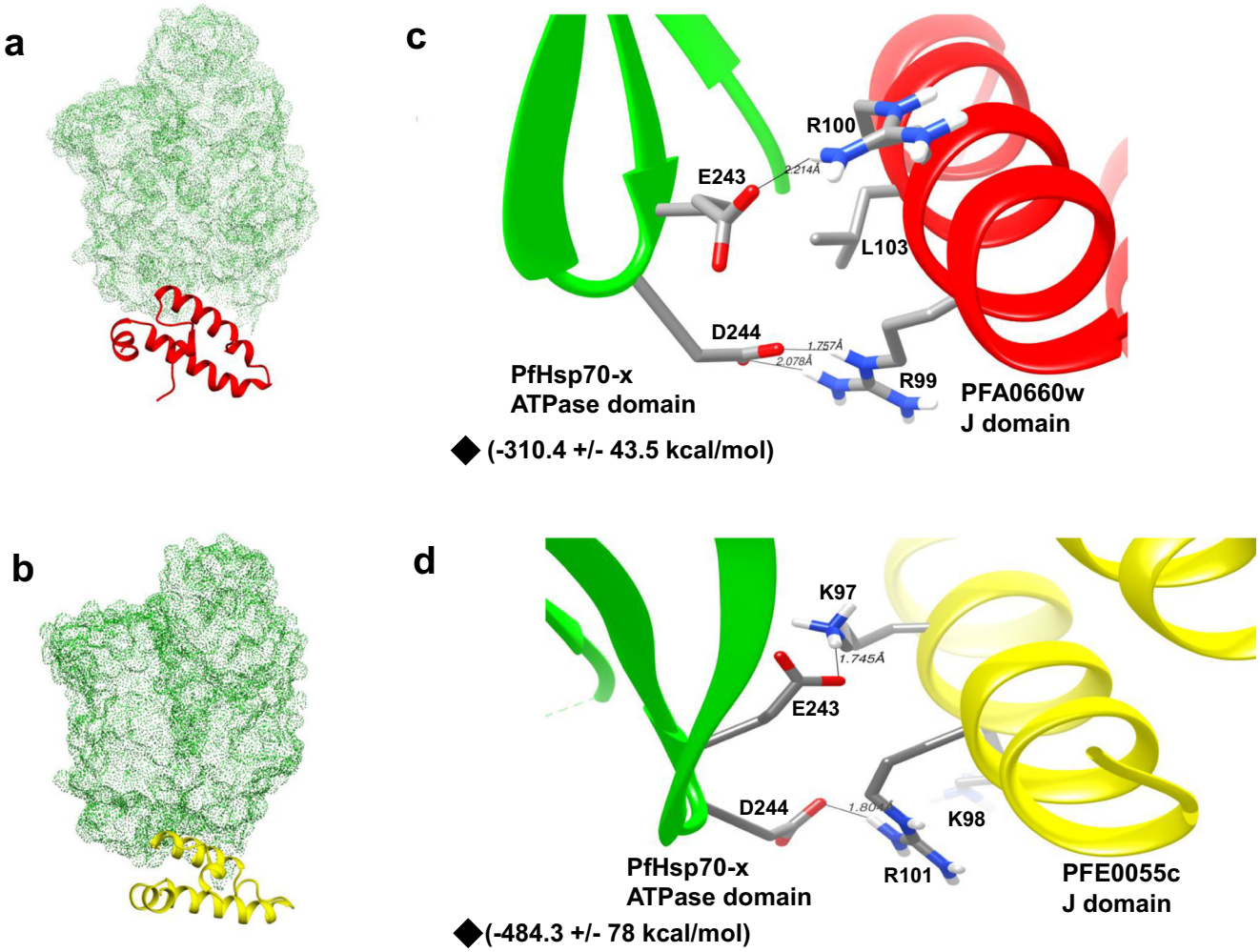

Fig. 4 Depth-cued 3D models of PFA0660w and PFE0055c showing proximity to the interactive surface of PfHsp70-x. (a) 3D representation of the best molecular docking pose between the J domain of PFA0660w and the ATPase domain of PfHsp70-x. PFA0660w is highlighted as red cartoons and PfHsp70-x as a green dotted surface. (b) 3D representation of the best molecular docking pose between the J domain of PFE0055c and the ATPase domain of PfHsp70-x. PFE0055c is highlighted as a yellow cartoon and PfHsp70-x as a green dotted surface. (c) Docked pose of the J domain of PFA0660w (red) with the ATPase domain of PfHsp70-x (green) in ribbon form with critical interacting residues (R99, R100, L103 in PFA0660w and E243, D244 in PfHsp70-x) focused and shown as sticks. (d) Docked pose of the J domain of PFE0055c (yellow) with the ATPase domain of PfHsp70-x (green) with critical interacting residues (K97, K98, R101 in PFE0055c and E243, D244 in PfHsp70-x) focused and shown as sticks. Hydrogen bonds have been represented as dotted lines and are labelled with respective distances. The red, blue, white, and grey colours represent oxygen, nitrogen, hydrogen, and carbon, respectively. ◆- Electrostatic binding energy. The molecular docking was conducted using HADDOCK2.2, and the graphical images were rendered using UCSF Chimera 1.10.1

Structural modelling indicated that the PFE0055c J domain-PfHsp70-x complex was more stable than that of PFA0660w

To get structural insights, we used the 3D crystallographic structure of the ATPase domain of PfHsp70-x (PDB ID: 6S02) and the J domain of PFA0660w (PDB ID: 6RZY), available at RSCB. The 3D structure for the PFE0055c J domain was modelled employing the aforementioned crystal structure of the PFA0660w J domain as a template. To gain a better understanding of the interactions of PFA0660w and PFE0055c with PfHsp70-x, molecular docking studies were carried out. The J domains of PFA0660w and PFE0055c were taken as ligands while the ATPase domain of PfHsp70-x was used as the receptor molecule. Docking provided best clusters for both of the J domains of PFA0660w and PFE0055c with the ATPase domain of PfHsp70-x, showing greater scores for the clusters of the PFE0055c J domain in comparison to the PFA0660w J domain (Online resource 1). Furthermore, for the best cluster (cluster 1), the molecular docking studies revealed that the electrostatic binding energy was higher for PFE0055c J domain-PfHsp70-x ATPase domain (− 484.3 ± 78 kcal/mol) in comparison to PFA0660w J domain-PfHsp70-x ATPase domain (− 310.4 ± 43.5 kcal/mol), suggesting stronger interaction between PFE0055c and PfHsp70-x. The best docked poses were visualized using UCSF Chimera (Fig. 4a

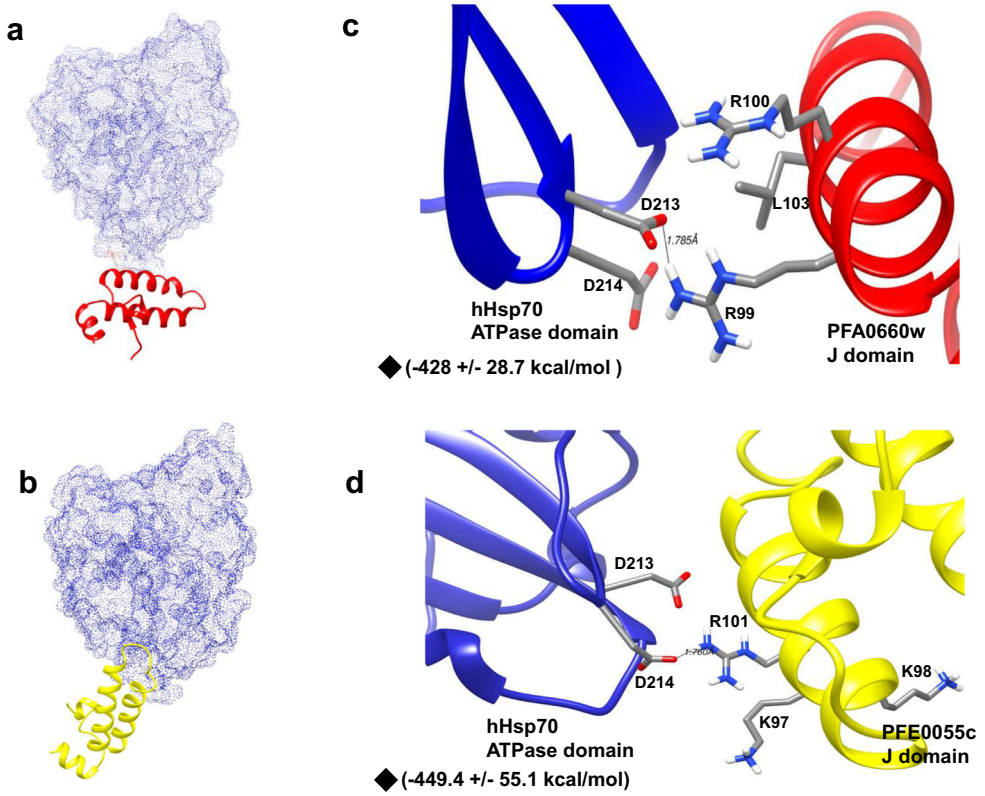

Fig. 5 Depth-cued 3D models of PFA0660w and PFE0055c showing proximity to the interactive surface of hHsp70. (a) 3D representation of the best molecular docking pose between the J domain of PFA0660w and the ATPase domain of hHsp70. PFA0660w is highlighted as red cartoons and hHsp70 as a blue dotted surface. (b) 3D representation of the best molecular docking pose between the J domain of PFE0055c and the ATPase domain of hHsp70. PFE0055c is highlighted as a yellow cartoon and hHsp70 as a blue dotted surface. (c) Docked pose of the J domain of PFA0660w (red) with the ATPase domain of hHsp70 (blue) in ribbon form with critical interacting residues (R99, R100, L103 in PFA0660w and D213, D214 in hHsp70) focused and shown as sticks. (d) Docked pose of the J domain of PFE0055c (yellow) with the ATPase domain of hHsp70 (blue) with critical interacting residues (K97, K98, R101 in PFE0055c and D213, D214 in hHsp70) focused and shown as sticks. Hydrogen bonds have been represented as dotted lines and are labelled with respective distances. The red, blue, white, and grey colours represent oxygen, nitrogen, hydrogen, and carbon, respectively. ◆- Electrostatic binding energy. The molecular docking was conducted using HADDOCK2.2, and the graphical images were rendered using UCSF Chimera 1.10.1

and b). Critical residues for J domain functionality, R99 and L103 (in PFA0660w) and K97 and R101 (in PFE0055c), were observed to be interacting with E243 and D244 in the ATPase domain of PfHsp70-x (Fig. 4c and d). To study the difference in interactions attributed due to these key residues, the ability to form hydrogen bonds was analysed. Interestingly, K97 and R101 in helix II of the J domain of PFE0055c appeared to adopt a pose that enabled strong hydrogen bonding with E243 and D244, respectively, of PfHsp70-x. On the other hand, helix II of PFA0660w appeared to adopt a less optimal pose in which R99 was making contact with D244, with L103 as would be expected making no contact with either E243 or D244, but rather a potential compensatory contact established between R100 and E243. Detailed interaction maps of binding sites for PFA0660w and PFE0055c with PfHsp70-x were obtained with LigPlot+, again illustrating that PFE0055c appeared to adopt a pose that allowed a stronger network of contacts than PFA0660w with PfHsp70-x (Online resource 3). Overall, these data suggested a higher degree of stability for the PFE0055c J domain-PfHsp70-x complex, compared to the PFA0660w J domain-PfHsp70-x complex (Fig. 4c and d). These findings are consistent with our earlier observations that PFE0055c was able to more effectively stimulate the basal ATPase activity of PfHsp70-x compared to PFA0660w.

Molecular interaction studies of the J domains of PFA0660w and PFE0055c (ligands) with the ATPase domain of hHsp70 (receptor; PDB ID: 1HJO) were performed, and the best docked poses were visualized using UCSF Chimera (Fig. 5a and b). Docking provided best clusters for both PFA0660w and PFE0055c interaction with hHsp70. The J domain of PFE0055c showed a greater score for all the clusters as compared to the J domain of PFA0660w (Online resource 2). The electrostatic binding energy for the top cluster of the PFA0660w J domain-hHsp70 ATPase domain and PFE0055c J domain-hHsp70 ATPase domain were – 428 ± 28.7 kcal/mol and − 449.4 ± 55.1 kcal/mol, respectively. Electrostatic binding energies were observed to be comparable for the J domains of

PFA0660w and PFE0055c which was also reflected in the similar fold stimulation of basal ATPase activity of hHsp70. Critical residues for J domain functionality, R99 and L103 (in PFA0660w) and K97 and R101 (in PFE0055c), were observed to be interacting with D213 and D214 in the ATPase domain of hHsp70 (equivalent to E243 and D244 in PfHsp70-x) (Fig. 5c and d). Helix II of the J domain of PFE0055c appeared to adopt a pose that enabled hydrogen bonding between R101 and D214 of hHsp70. On the other hand, helix II of PFA0660w appeared to adopt a pose in which R99 was making contact with D213 of hHsp70, perhaps compensating for the lack of contact between L103 and either D213 or D214 of hHsp70. Detailed interaction maps of the binding sites for the PFA0660w J domain and the PFE0055c J domain with the hHsp70 ATPase domain were obtained with LigPlot+ (Online resource 4).

Electrostatic binding energy comparison for PFE0055c J domain-PfHsp70-x ATPase domain (−484.3 ± 78 kcal/mol) with PFE0055c J domain-hHsp70 ATPase domain (−449.4 ± 55.1 kcal/mol) showed that PFE0055c interacted with PfHsp70-x to a slightly greater extent than hHsp70 (Online resources 1 and 2). This only partially correlated with our biochemical characterization, since we showed that PFE0055c stimulated PfHsp70-x to a substantially greater extent than hHsp70. This may reflect the limitations of the in silico methodology to analyse structural differences, particularly the lack of factoring in the contributions of binding by domains beyond the J domain-ATPase domain region; which needs to be considered and studied in the future.

It is worth noting that K26 of EcDnaJ (positionally equivalent to R101 of PFE0055c and L103 of PFA0660w; Fig. 1a and b) interacts with E217 in EcDnaK. Interestingly, E217 of EcDnaK is positionally equivalent to E248 in PfHsp70-x and not E243 or D244 (although they could be topologically equivalent). Our detailed contact analysis (Online resource 3) indicated that K98 of the PFE0055c J domain interacted with E248 of PfHsp70-x. While we cannot exclude that there may be topological equivalence, our modelling suggests that there are some differences in the network of contacts for the parasitic system compared to the bacterial system.

Conclusion

To our knowledge, this is the first study to provide evidence that the exported type II PfJDP, PFE0055c, serves as a specific co-chaperone of the exported PfHsp70-x. PFE0055c stimulated the basal ATPase activity of PfHsp70-x by at least threefold, and this enhancement was inhibited by C86, indicating that the interaction was J domain–based. Structural analyses indicated that PFE0055c formed a more stable complex with PfHsp70-x than did PFA0660w. Since derivatives of chalcones and benzothiazole rhodacyanines have been shown to have antimalarial activity, these structural and small molecule inhibitor studies on PFE0055c and PfHsp70-x open up new avenues for antimalarial drug discovery.

Supplementary Information The online version contains supplementary material available at https://doi.org/10.1007/s12192-020-01181-2.

Acknowledgements Financial assistance from The University of Notre Dame Australia is gratefully acknowledged. We acknowledge Assoc. Prof. Mark Watson for providing laboratory management and technical support at The Institute for Immunology and Infectious Disease, Murdoch University, WA, Australia. We are grateful to Dr. Eva-Rachele Pesce for the technical assistance in the development of certain reagents used in this study.

Authors' contributions Gregory L. Blatch and Tanima Dutta contributed to the study conception and design. Material preparation, data collection, and analysis were performed by Tanima Dutta and Gregory L. Blatch. Resource materials (small molecule inhibitors) were provided for research by Jason E. Gestwicki. Bioinformatics models were conceptualized by Gregory L. Blatch and developed by Harpreet Singh. The manuscript was written by Tanima Dutta and reviewed by Jason E. Gestwicki and Gregory L. Blatch. All authors commented on versions of the manuscript. All authors read and approved the final manuscript.

Funding Financial assistance is received from The University of Notre Dame, Fremantle, Australia.

Data availability Yes, all the data and material are original and available.

Compliance with ethical standards

Conflict of interest No conflict of interest.

Ethics approval Not applicable.

Consent to participate Not applicable.

Consent for publication Publication agreement application attached.

Code availability Not applicable.

References

Ahmad A, Bhattacharya A, McDonald RA et al (2011) Heat shock protein 70 kDa chaperone/DnaJ cochaperone complex employs an unusual dynamic interface. PNAS 108:18966–18971

Akide-Ndunge OB, Tambini E, Giribaldi G, McMillan PJ, Müller S, Arese P, Turrini F (2009) Co-ordinated stage-dependent enhancement of *Plasmodium falciparum* antioxidant enzymes and heat shock protein expression in parasites growing in oxidatively stressed or G6PD-deficient red blood cells. Malar J 8:113

Anas M, Shukla A, Tripathi A, Kumari V, Prakash C, Nag P, Kumar LS, Sharma SK, Ramachandran R, Kumar N (2020) Structural–functional diversity of malaria parasite's PfHSP70-1 and PfHSP40 chaperone pair gives an edge over human orthologs in chaperone-assisted protein folding. Biochem J 477:3625–3643

Behl A, Kumar V, Bisht A, Panda JJ, Hora R, Mishra PC (2019) Cholesterol bound *Plasmodium falciparum* co-chaperone

'PFA0660w'complexes with major virulence factor 'PfEMP1'via chaperone 'PfHsp70-x'. Sci Rep 9:1–7

Bondos SE, Bicknell A (2003) Detection and prevention of protein aggregation before, during, and after purification. Anal Biochem 316: 223–231

Botha M, Pesce ER, Blatch GL (2007) The Hsp40 proteins of *Plasmodium falciparum* and other Apicomplexa: regulating chaperone power in the parasite and the host. Int J Biochem Cell Biol 39: 1781–1803

Botha M, Chiang AN, Needham PG, Stephens LL, Hoppe HC, Külzer S, Przyborski JM, Lingelbach K, Wipf P, Brodsky JL, Shonhai A, Blatch GL (2011) *Plasmodium falciparum* encodes a single cytosolic type I Hsp40 that functionally interacts with Hsp70 and is upregulated by heat shock. Cell Stress Chaperon 16:389–401

Bradford MM (1976) A rapid and sensitive method for the quantitation of microgram quantities of protein utilizing the principle of protein-dye binding. Anal Biochem 72:248–254

Charnaud SC, Dixon MWA, Nie CQ, Chappell L, Sanders PR, Nebl T, Hanssen E, Berriman M, Chan JA, Blanch AJ, Beeson JG, Rayner JC, Przyborski JM, Tilley L, Crabb BS, Gilson PR (2017) The exported chaperone Hsp70-x supports virulence functions for *Plasmodium falciparum* blood stage parasites. PLoS One 12: e0181656

Cheetham ME, Caplan AJ (1998) Structure, function and evolution of DnaJ: conservation and adaptation of chaperone function. Cell Stress Chaperon 3:28–36

Cheetham ME, Jackson AP, Anderton BH (1994) Regulation of 70-kDa heat-shock-protein ATPase activity and substrate binding by human DnaJ-like proteins, HSJ1a and HSJ1b. Eur J Biochem 226:99–107

Chiang AN, Valderramos JC, Balachandran R, Chovatiya RJ, Mead BP, Schneider C, Bell SL, Klein MG, Huryn DM, Chen XS, Day BW, Fidock DA, Wipf P, Brodsky JL (2009) Select pyrimidinones inhibit the propagation of the malarial parasite, *Plasmodium falciparum*. Bioorg Med Chem 17:1527–1533

Cockburn IL, Pesce ER, Pryzborski JM, Davies-Coleman MT, Clark PG, Keyzers RA, Stephens LL, Blatch GL (2011) Screening for small molecule modulators of Hsp70 chaperone activity using protein aggregation suppression assays: inhibition of the plasmodial chaperone PfHsp70-1. Biol Chem 392:431–438

Cockburn IL, Boshoff A, Pesce ER, Blatch GL (2014) Selective modulation of plasmodial Hsp70s by small molecules with antimalarial activity. Biol Chem 395:1353–1362

Cyr DM, Ramos CH (2015) Specification of Hsp70 function by type I and type II Hsp40. In: The networking of chaperones by co-chaperones. Springer, Cham, pp 91–102

Daniyan MO, Blatch GL (2017) Plasmodial Hsp40s: new avenues for antimalarial drug discovery. Curr Pharm Des 23:4555–4570

Daniyan MO, Boshoff A, Prinsloo E, Pesce ER, Blatch GL (2016) The malarial exported PFA0660w is an Hsp40 co-chaperone of PfHsp70-x. PLoS One 11:e0148517

Day J, Passecker A, Beck HP, Vakonakis I (2019) The *Plasmodium falciparum* Hsp70-x chaperone assists the heat stress response of the malaria parasite. FASEB J 33:14611–14624

Fan CY, Lee S, Cyr DM (2003) Mechanisms for regulation of Hsp70 function by Hsp40. Cell Stress Chaperon 8:309–316

Gässler CS, Buchberger A, Laufen T et al (1998) Mutations in the DnaK chaperone affecting interaction with the DnaJ cochaperone. PNAS 95:15229–15234

Genevaux P, Schwager F, Georgopoulos C, Kelley WL (2002) Scanning mutagenesis identifies amino acid residues essential for the in vivo activity of the *Escherichia coli* DnaJ (Hsp40) J-domain. Genetics 162:1045–1053

Gestwicki JE, Shao H (2019) Inhibitors and chemical probes for molecular chaperone networks. J Biol Chem 294:2151–2161

Gillies AT, Taylor R, Gestwicki JE (2012) Synthetic lethal interactions in yeast reveal functional roles of J protein co-chaperones. Mol BioSyst 8:2901–2908

Grover M, Chaubey S, Ranade S, Tatu U (2013) Identification of an exported heat shock protein 70 in Plasmodium falciparum. Parasite 20:2

Hatherley R, Blatch GL, Bishop ÖT (2014) *Plasmodium falciparum* Hsp70-x: a heat shock protein at the host–parasite interface. J Biomol Struct Dyn 32:1766–1779

Hennessy F, Cheetham ME, Dirr HW, Blatch GL (2000) Analysis of the levels of conservation of the J domain among the various types of DnaJ-like proteins. Cell Stress Chaperon 5:347–358

Hennessy F, Boshoff A, Blatch GL (2005a) Rational mutagenesis of a 40 kDa heat shock protein from *Agrobacterium tumefaciens* identifies amino acid residues critical to its in vivo function. Int J Biochem Cell Biol 37:177–191

Hennessy F, Nicoll WS, Zimmermann R, Cheetham ME, Blatch GL (2005b) Not all J domains are created equal: implications for the specificity of Hsp40-Hsp70 interactions. Protein Sci 14:1697–1709

Jha P, Laskar S, Dubey S, Bhattacharyya MK, Bhattacharyya S (2017) *Plasmodium* Hsp40 and human Hsp70: a potential cochaperone-chaperone complex. Mol Biochem Parasitol 214:10–13

Kampinga HH, Craig EA (2010) The HSP70 chaperone machinery: J proteins as drivers of functional specificity. Nat Rev Mol Cell Biol 11:579–592

Kampinga HH, Andreasson C, Barducci A, Cheetham ME, Cyr D, Emanuelsson C, Genevaux P, Gestwicki JE, Goloubinoff P, Huerta-Cepas J, Kirstein J, Liberek K, Mayer MP, Nagata K, Nillegoda NB, Pulido P, Ramos C, de los Rios P, Rospert S, Rosenzweig R, Sahi C, Taipale M, Tomiczek B, Ushioda R, Young JC, Zimmermann R, Zylicz A, Zylicz M, Craig EA, Marszalek J (2019) Function, evolution, and structure of J-domain proteins. Cell Stress Chaperon 24:7–15

Kityk R, Kopp J, Mayer MP (2018) Molecular mechanism of J-domain-triggered ATP hydrolysis by Hsp70 chaperones. Mol Cell 69:227–237

Külzer S, Rug M, Brinkmann K, Cannon P, Cowman A, Lingelbach K, Blatch GL, Maier AG, Przyborski JM (2010) Parasite-encoded Hsp40 proteins define novel mobile structures in the cytosol of the P. falciparum-infected erythrocyte. Cell Microbiol 12:1398–1420

Külzer S, Charnaud S, Dagan T, Riedel J, Mandal P, Pesce ER, Blatch GL, Crabb BS, Gilson PR, Przyborski JM (2012) *Plasmodium falciparum*-encoded exported hsp70/hsp40 chaperone/co-chaperone complexes within the host erythrocyte. Cell Microbiol 14:1784–1795

Kumar DP, Vorvis C, Sarbeng EB, Ledesma VC, Willis JE, Liu Q (2011) The four hydrophobic residues on the Hsp70 inter-domain linker have two distinct roles. J Mol Biol 411:1099–1113

Laskowski RA, Swindells MB (2011) LigPlot+: multiple ligand-protein interaction diagrams for drug discovery. J Chem Inf Model 51: 2778–2786

Mayer MP, Bukau B (2005) Hsp70 chaperones: cellular functions and molecular mechanism. Cell Mol Life Sci 62:670–684

Mayer MP, Laufen T, Paal K, McCarty JS, Bukau B (1999) Investigation of the interaction between DnaK and DnaJ by surface plasmon resonance spectroscopy. J Mol Biol 289:1131–1144

Moses MA, Kim YS, Rivera-Marquez GM et al (2018) Targeting the Hsp40/Hsp70 chaperone axis as a novel strategy to treat castration-resistant prostate cancer. Cancer Res 78:4022–4035

Nicoll WS, Botha M, McNamara C, Schlange M, Pesce ER, Boshoff A, Ludewig MH, Zimmermann R, Cheetham ME, Chapple JP, Blatch GL (2007) Cytosolic and ER J-domains of mammalian and parasitic origin can functionally interact with DnaK. Int J Biochem Cell Biol 39:736–751

Njunge JM, Ludewig MH, Boshoff A, Pesce ER, Blatch GL (2013) Hsp70s and J proteins of *Plasmodium* parasites infecting rodents

and primates: structure, function, clinical relevance, and drug targets. Curr Pharm Des 19:387–403

Njunge JM, Mandal P, Przyborski JM, Boshoff A, Pesce ER, Blatch GL (2015) PFB0595w is a *Plasmodium falciparum* J protein that co-localizes with PfHsp70-1 and can stimulate its in vitro ATP hydrolysis activity. Int J Biochem Cell Biol 62:47–53

Pesce ER, Blatch GL (2014) Plasmodial Hsp40 and Hsp70 chaperones: current and future perspectives. Parasitol 141:1167–1176

Pesce ER, Acharya P, Tatu U, Nicoll WS, Shonhai A, Hoppe HC, Blatch GL (2008) The *Plasmodium falciparum* heat shock protein 40, Pfj4, associates with heat shock protein 70 and shows similar heat induction and localization patterns. Int J Biochem Cell Biol 40:2914–2926

Pesce ER, Cockburn IL, Goble JL, Stephens LL, Blatch GL (2010) Malaria heat shock proteins: drug targets that chaperone other drug targets. Infect Disord Drug Targets (Formerly Current Drug Targets-Infectious Disorders) 10:147–157

Pettersen EF, Goddard TD, Huang CC, Couch GS, Greenblatt DM, Meng EC, Ferrin TE (2004) UCSF chimera - a visualization system for exploratory research and analysis. J Comp Chem 25:1605–1612

Przyborski JM, Diehl M, Blatch GL (2015) Plasmodial HSP70s are functionally adapted to the malaria parasite life cycle. Front Mol Biosc 2:34

Pudhom K, Kasai K, Terauchi H, Inoue H, Kaiser M, Brun R, Ihara M, Takasu K (2006) Synthesis of three classes of rhodacyanine dyes and evaluation of their in vitro and in vivo antimalarial activity. Bioorg Med Chem 14:8550–8563

Qin HL, Zhang ZW, Lekkala R, Alsulami H, Rakesh KP (2020) Chalcone hybrids as privileged scaffolds in antimalarial drug discovery: a key review. Eur J Med Chem 193:112215

Rinaldi S, Assimon VA, Young ZT, Morra G, Shao H, Taylor IR, Gestwicki JE, Colombo G (2018) A local allosteric network in heat shock protein 70 (Hsp70) links inhibitor binding to enzyme activity and distal protein–protein interactions. ACS Chem Biol 13:3142–3152

Sambrook J, Russell DW (2001) Molecular cloning: a laboratory manual. Cold Spring Harbor Laboratory Press, Cold Spring Harbor, New York

Shao H, Li X, Moses MA, Gilbert LA, Kalyanaraman C, Young ZT, Chernova M, Journey SN, Weissman JS, Hann B, Jacobson MP, Neckers L, Gestwicki JE (2018) Exploration of benzothiazole rhodacyanines as allosteric inhibitors of protein–protein interactions with heat shock protein 70 (Hsp70). J Med Chem 61:6163–6177

Shonhai A, Boshoff A, Blatch GL (2007) The structural and functional diversity of Hsp70 proteins from *Plasmodium falciparum*. Protein Sci 16:1803–1818

Shonhai A, Maier AG, Przyborski JM, Blatch GL (2011) Intracellular protozoan parasites of humans: the role of molecular chaperones in development and pathogenesis. Protein Peptide Lett 18:143–157

Sinha S, Batovska DI, Medhi B, Radotra BD, Bhalla A, Markova N (2019) In vitro anti-malarial efficacy of chalcones: cytotoxicity profile, mechanism of action and their effect on erythrocytes. Malar J 18:421

Swietnicki W (2006) Folding aggregated proteins into functionally active forms. Curr Opin Biotechnol 17:367–372

Tsai J, Douglas MG (1996) A conserved HPD sequence of the J-domain is necessary for YDJ1 stimulation of Hsp70 ATPase activity at a site distinct from substrate binding. J Biol Chem 271:9347–9354

Van Zundert GC, Rodrigues JP, Trellet M et al (2016) The HADDOCK2.2 web server: user-friendly integrative modeling of biomolecular complexes. J Mol Biol 428:720–725

World Health Organization (2018) World malaria report 2018. World Health Organization. https://apps.who.int/iris/handle/10665/275867